Published in final edited form as:
J Am Chem Soc. 2006 June 21; 128(24): 7938–7946. doi:10.1021/ja0612854.

Local Heating of Discrete Droplets Using Magnetic Porous Silicon-Based Photonic Crystals

Ji-Ho Park[1,2], **Austin M. Derfus**[3], **Ester Segal**[1], **Kenneth S. Vecchio**[2], **Sangeeta N. Bhatia**[3,4], and **Michael J. Sailor**[1,2,*]

[1]Department of Chemistry and Biochemistry, University of California, San Diego, 9500 Gilman Drive, La Jolla, CA 92093-0358, USA

[2]Materials Science and Engineering Program, University of California, San Diego, 9500 Gilman Drive, La Jolla, CA 92093-0411, USA

[3]Department of Bioengineering, University of California, San Diego, 9500 Gilman Drive, La Jolla, CA 92093-0412, USA

[4]Division of Health Sciences and Technology (Harvard-MIT) and Department of Electrical Engineering and Computer Science, Massachusetts Institute of Technology, 77 Massachusetts Avenue, Bldg. E19-502d, Cambridge, MA 02139, USA

Abstract

This paper describes a method for local heating of discrete micro-liter scale liquid droplets. The droplets are covered with magnetic porous Si microparticles, and heating is achieved by application of an external alternating electromagnetic field. The magnetic porous Si microparticles consist of two layers: the top layer contains a photonic code and it is hydrophobic, with surface-grafted dodecyl moieties. The bottom layer consists of a hydrophilic Si oxide host layer that is infused with Fe_3O_4 nanoparticles. The amphiphilic microparticles spontaneously align at the interface of a water droplet immersed in mineral oil, allowing manipulation of the droplets by application of a magnetic field. Application of an oscillating magnetic field (338 kHz, 18A RMS current in a coil surrounding the experiment) generates heat in the superparamagnetic particles that can raise the temperature of the enclosed water droplet to >80 °C within 5 min.

A simple microfluidics application is demonstrated: combining complementary DNA strands contained in separate droplets and then thermally inducing dehybridization of the conjugate. The complementary oligonucleotides were conjugated with the cyanine dye fluorophores Cy3 and Cy5 to quantify the melting/re-binding reaction by fluorescence resonance energy transfer (FRET). The magnetic porous Si microparticles were prepared as photonic crystals, containing spectral codes that allowed the identification of the droplets by reflectivity spectroscopy. The technique demonstrates the feasibility of tagging, manipulating, and heating small volumes of liquids without the use of conventional microfluidic channel and heating systems.

Keywords

fluorescence resonance energy transfer (FRET); lab-on-a-chip; magnetically induced heating; microfluidics; photonic crystal; porous silicon

*Correspondence should be addressed to M.J.S. (msailor@ucsd.edu).

Introduction

Much of the work on microfluidics to date has involved production of patterned fluidic circuits consisting of microchannels.[1–7] An alternative approach involves the manipulation of discrete droplets rather than continuous liquid streams.[8–13] Through independent micro-manipulation of discrete droplets, complex procedures can be carried out in a manner that directly mimics traditional bench-top protocols. Because each droplet can be independently controlled, highly integrated, scalable and flexible architectures can be implemented.[10] A number of techniques have been described for the actuation of droplets on solid surfaces including the use of thermocapillary effects,[14] photochemical effects,[15] electrochemical gradients,[16] surface tension gradients,[17] temperature gradients,[18] air pressure,[19] structured surfaces,[20] dielectrophoresis,[21] and electrostatic methods.[8]

An extension of this approach is a liquid-liquid microfluidic system for manipulating freely suspended microliter or nanoliter droplets. Only few such systems have been reported to date and new manipulation methods continue to emerge.[22] Pollack et al.[8] have demonstrated the electrowetting-based transport of aqueous electrolyte droplets in a silicone oil media using a two-sided open-channel planar microactuator structure. Velev et al.[9,23] described a system in which water or dodecene microdroplets float freely on a surface of fluorinated oil and electric fields are applied through an array of electrodes below the surface of the oil phase to manipulate the droplets. Kotz et al.[7,24] have demonstrated that asymmetric laser heating of the liquid/liquid interface between an aqueous droplet and its surrounding immiscible fluid can induce thermal Marangoni flows to move the droplet, and the utility of the method was demonstrated with a protein assay. Recently, we demonstrated the manipulation and identification of liquid droplets using amphiphilic, magnetic, one-dimensional photonic crystal chaperones, made from porous Si.[25] The chaperones align themselves at the interface of an aqueous droplet immersed in an organic medium and application of an external magnetic field allows transport of the droplet. Furthermore, the optical reflectivity spectrum of the photonic crystal displays a peak that serves to identify the droplet. The coated droplets can be coalesced with other droplets under the influence of a magnetic field to perform simple microreactions.

A key requirement for many biological and chemical reactions is efficient heating of the sample. For example, the ability to perform the polymerase chain reaction (PCR) with high efficiency in microfluidic environments is critically dependent on rapid and precise heat transfer.[2] Non-zonal heating is generally accomplished using a Peltier device,[26] a thin film heater[27] or a laboratory hotplate.[28] Accurate zonal heating may be achieved through the use of complex on-chip resistive heater networks, requiring additional fabrication steps.[29] The primary restriction associated with these heating methods is the thermal properties and mass of the heating block and the reaction chamber, which ultimately limit the rate at which the sample can be heated and cooled.[30,31] The thermal mass problem can be eliminated by using non-contact heating methods to specifically heat the sample or the reaction medium.[30,32] All the heating techniques described above have been developed for microchannel-based microfluidics and also have been implemented in droplet-based microfluidics. However, advanced droplet-based microfludics requires efficient localized heating of the individual droplets with minimal heat transfer to the surroundings.

The present paper describes a method for precise local heating of small liquid volumes using magnetic amphiphilic porous Si microparticles. The magnetic properties of the magentite particles infused within one layer of the bifunctional porous Si microparticles are utilized for heat generation by application of an alternating radio frequency (RF) electromagnetic field. The feasibility of this heating concept in performing microreactions is demonstrated by

melting complementary oligonucleotides conjugated with dye molecules, while monitoring the dehybridization in real time using fluorescence resonance energy transfer (FRET).

Experimental

Materials

All reagents were used as received. Aqueous HF (48%) and ethanol (99.9%) were supplied by Fisher Scientific and AAper, respectively. 1-dodecene (95%) was supplied by Sigma-Aldrich. Porous Si samples were prepared with single-crystalline highly-doped p-type Si wafers from Siltronix Corp. (0.0008 Ω-cm resistivity, ‹100› oriented, B-doped).

Preparation of Amphiphilic Optically Encoded Porous Silicon Films

Porous Si samples were prepared by anodization of a highly-doped p-type Si wafer in ethanolic HF solution (3:1 (v/v) 48% aqueous HF:ethanol) using a platinum mesh counter-electrode. CAUTION: hydrofluoric acid is toxic and highly irritating to the skin; prompt medical attention should be obtained if the liquid contacts the skin or if the vapors are inhaled. Si wafers with an exposed area of 1.33 cm^2 were contacted on the back side with a strip of aluminum foil and mounted in a Teflon etching cell. Two layers were prepared in each sample; one is referred to as the “encoding” layer and the other is the “host” layer, intended to contain magnetite nanoparticles. The “encoding” layer was prepared as a one-dimensional photonic crystal using the waveform superposition method previously described.[33] Two types of samples were prepared for encoding purposes: (1) a “one peak” rugate filter was etched using a sinusoidal current waveform oscillating between 11.3 and 56.8 mA/cm^2, the frequency of the waveform was 0.18 s^{-1}, repeated for 400 s in a 3:1 (v/v) ethanolic HF solution; (2) a “three peak” sample was etched using a current waveform composed of three sine waves with frequencies of 1.5, 1.6, and 1.7 s^{-1} for 400 s in 3:1 (v/v) ethanolic HF solution. After etching, the sample was rinsed with ethanol several times and then dried under a stream of nitrogen. Thermal hydrosilylation was accomplished by placing the porous Si sample in liquid 1-dodecene in a Schlenk flask, degassing the liquid with three successive freeze-pump-thaw cycles, and then heating at 140 °C under nitrogen for two hours [25,34]. After removal of the solution, samples were rinsed with ethanol and acetone several times and dried under a stream of nitrogen. The “host” layer (for magnetite nanoparticles) was then etched into the substrate, immediately beneath the encoding layer, using a constant current density of 303 mA/cm^2 for 200 s in the same ethanolic HF etching solution. The double-layered porous Si film was then removed from the crystalline Si substrate by applying a current pulse of ca. 15 mA/cm^2 in a 3.3% (v/v) ethanolic HF solution. After removal of the etching solution, the freestanding porous Si film was rinsed with ethanol and acetone several times and then dried under a stream of nitrogen.

Preparation of Magnetized Amphiphilic Encoded Porous Silicon Microparticles

A magnetite (Fe_3O_4) colloidal suspension with a mean particle size of 10 nm (measured by Transmission Electron Microscopy) was prepared using a previously described method.[35] The magnetite suspension was mixed with acetone at a ratio of 1:3 (v/v). The concentration of the final magnetite suspension was approx. 1 mg/mL. The porous Si film (with its host layer side facing up) was placed in the center of an aluminum weighing dish and a strong magnet was located under the dish. A volume of 0.5 mL of the magnetite nanoparticle suspension was added on top of the film. When the solution evaporated, the magnetized film was rinsed thoroughly with ethanol and acetone several times and then dried in air. The film was then thermally oxidized at 100 °C overnight. The thermally oxidized film was fractured to micron-sized particles by ultrasonication (20 s) in acetone. The resulting magnetic porous Si microparticles were rinsed with ethanol and acetone several times and then filtered using a 100 μm filter to remove free magnetite nanoparticles and small aggregates. The

magnetized porous Si particles were separated from the non-magnetized particles with a NdFeB rare earth magnet (National Imports NSN0550, 3.18 mm diameter and 25.40 mm length, grade N40). The final size of the magnetic porous Si microparticles was 150~200 μm.

Scanning Electron Microscopy

Scanning electron microscope (SEM) images of the cross section of the magnetized porous Si film were obtained using a FEI Quanta 600 environmental scanning electron microscope equipped with an EDS Oxford ELX II apparatus and a four-sector back-scattered electron detector.

Measurement of Magnetic Properties

Magnetic properties were investigated using a Quantum Design MPMS2 SQUID magnetometer with fields up to 5000 Oe at 300 K. Measurements were performed on magnetite nanoparticles, porous Si particles, and magnetite-infused porous Si particles. The amount of magnetite nanoparticles infused into the porous Si host layer was quantified by dissolving the host matrix in an aqueous solution containing 5M NaOH and ~10% ethanol at room temperature overnight. The residue was filtered, dried, and weighed. It was assumed that the residue is composed of an agglomeration of magnetite nanoparticles. Three samples were used for the dissolution tests and the measurements were averaged. These numbers were then compared with the magnetometer results.

Measurement of Interferomeric Reflectance Spectra

Interferometric reflectance spectra of encoded magnetic porous Si microparticles surrounding an aqueous droplet immersed in oil were collected using an Ocean Optics CCD S-2000 spectrometer fitted with a microscope objective lens coupled to a bifurcated fiber optic cable. A tungsten light source was focused (spot size approx. 1 mm^2) onto the magnetic porous Si microparticles located at the droplet/oil interface. Reflectivity data were recorded in the wavelength range 400–1000 nm, with a spectral acquisition time of 100 ms. Both illumination of the surface and detection of the reflected light were performed along an axis coincident with a vector normal to the droplet/oil interface.

Radiofrequency Electromagnetic Field-Induced Heating

Alternating electromagnetic fields were generated by applying an alternating current to a coil with 2 turns and a cross section of ~ 70 mm^2. The coils were wrapped around a Petri dish containing the aqueous droplets suspended in oil. The Petri dish had a depression in its center in order to fix the droplet in one place. A power supply (Ameritherm Nova 3) was used to apply alternating electromagnetic fields resonating at 338 kHz. Maximum power (3kW) was used for most experiments (equivalent to 18 Amps RMS through the coil). During the experiments, cooling water (15 °C) was circulated through the coil to avoid overheating of the coil. The temperature within the droplet was measured using a metallic K-type thermocouple probe, inserted immediately after the coil power was switched off.

Fluorescence Resonance Energy Transfer (FRET) Assay

All fluorophore-conjugated DNA oligonucleotides for the FRET assay were obtained from Integrated DNA Technologies, Inc. The sequence of the Cy3-conjugated oligonucleotide was 5′ Cy3 TGA TTC AAG CCG ACT 3′, and the Cy5-conjugated oligonucleotide was 5′ AGT CGG CTT GAA TCA Cy5 3′. The melting temperature for the pair was calculated to be 46.8°C in 50 mM NaCl.

Droplet #1 (D1) contained 0.6 nmole of Cy3-oligonucleotides in a volume of 25 μL of buffer solution and was partially covered with the “one peak”-encoded magnetic porous Si microparticles (~2 mg). Droplet #2 (D2) contained 0.6 nmole of Cy5-oligonucleotides in a volume of 25 μL of buffer and was covered with the “three peak”-encoded magnetic porous Si microparticles (~2 mg). The aqueous buffer used in the droplets contained ultra-pure water (Sigma-Aldrich) and Dulbecco’s phosphate buffered saline (DPBS without calcium and magnesium, Sigma-Aldrich) with a composition of 54.4 mM NaCl, 1.1 mM KCl, 3.2 mM Na_2HPO_4 and 0.6 mM KH_2PO_4. These encoded droplets were placed in mineral oil (Sigma-Aldrich) within the experimental dish. Using a magnet, the Cy3 droplet was moved and merged with the Cy5 droplet located in the center of the experimental dish. The mixed droplet, partially covered with the magnetic porous Si microparticles (~4 mg), was heated in 0.5 mL of mineral oil with an alternating electromagnetic field (3 kW) while the photoluminescence spectrum was monitored for FRET.

Fluorescence Measurements

The steady-state photoluminescence (PL) spectra of FRET from the droplet were obtained with an Acton 0.275 m monochromator, 500 nm-cutoff filter, and a UV-enhanced liquid nitrogen-cooled, charge-coupled device (CCD) detector (Princeton Instruments) fitted with a microscope objective lens coupled to fiber optic cable. Blue light with an emission wavelength range of 470 ± 20 nm (150 watts, Illumatool Bright Light System LT-9900, Lightools Research) was used as the excitation source and routed through two flexible fiber-optic cables. The light source and detector lens were located at a distance of ~12 cm from the top of the droplet to prevent any heat generation in the metallic materials of the detector and light source. Fluorescence measurements were obtained normal to the droplet/dish (with the two excitation sources at ~45 degrees from normal), and integrated for 2 s.

The relationship between temperature and fluorescence measured using RF field-induced heating was compared with that observed when the droplet/oil apparatus was heated with a laboratory hotplate. The experimental dish containing the FRET probe-loaded droplet described above was placed on top of a 100 mL beaker of water and heated to 60 °C. The hotplate was removed and fluorescence spectra were obtained at 1 °C intervals as the droplet cooled to 35 °C. The beaker containing 100 mL of water was used as a heat reservoir to slow the cooling rate to approximately 0.5 °C per minute. Temperature of the droplet was monitored continuously with a thermocouple probe.

Results and Discussion

Preparation and Characterization of Magnetized Amphiphilic Porous Si Microparticles

The synthesis scheme followed to produce magnetic amphiphilic porous Si microparticles is outlined in Fig. 1. A multilayered porous Si dielectric mirror, referred to as the encoding layer, is first electrochemically etched into the (100) face of a single-crystal, p-type Si wafer using a temporally modulated current waveform. The variation in refractive index resulting from the modulated etch produces sharp resonance features in the optical reflectivity spectrum of the film, whose wavelengths are determined by the characteristic frequency components of the modulated current waveform.[33] The film is then thermally hydrosilylated with 1-dodecene, following published procedures,[25,34] to generate a chemically stable hydrophobic layer. A second porous layer, to act as a host for magnetite nanoparticles, is etched into the substrate immediately beneath the encoding layer. The etching conditions for the host layer were optimized to create relatively large and cylindrically-shaped pores to accommodate the magnetite nanoparticles with a mean size of 10 nm. The electron microscope image of a porous Si microparticle (Fig. 2a) reveals an average pore size of ~50 nm for the host layer while the pore size of the encoding layer is less than 10 nm.

After etching, the double-layered structure is removed from the Si substrate by application of a current pulse. The host layer is then infused with magnetite (Fe_3O_4) nanoparticles. The magnetite concentration within the porous Si particles is critical not only to allow manipulation of the droplets[25] but also to allow efficient heat generation when subjected to an alternating electromagnetic field. A highly concentrated acetone dispersion of magnetite nanoparticles (mean particle diameter of 10 nm[35]) is infiltrated into the host layer using a strong rare-earth magnet located under the porous Si film. The solvent is then evaporated while the sample is maintained in the magnetic field. It is suggested that the magnetic field and the interfacial capillary forces generated during evaporation of the solvent[36] results in enhanced infusion of the magnetic nanoparticles into the porous structure. Moreover, the surfactant tetramethyl ammonium hydroxide (TMAOH) present in the magnetite nanoparticle dispersion is often used for anisotropic etching of Si.[37] Thus, the surfactant may further enhance the infusion and entrapment of the magnetite nanoparticles within the structure by slightly etching the porous Si host layer. The encoding layer is protected from chemical attack by the passivating dodecene surface modification step.

The magnetite infiltration step is followed by thermal oxidation to further trap the nanoparticles in the Si matrix.[25] Thermal oxidation preferentially produces oxide on the more reactive, hydrogen-terminated host layer compared with the chemically stable, hydrosilylated encoding layer. The oxide imparts hydrophilic character to the layer, whereas the hydrosilylated side retains its hydrophobic nature, allowing the particles to align at an aqueous/organic liquid interface. The infiltration of magnetite (iron oxide) nanoparticles in the porous Si host layer is confirmed by energy dispersive X-ray spectroscopy (EDS). An elemental line scan for iron and oxygen obtained along the cross-section of a magnetic porous Si micoparticle (shown superimposed over the backscattered-electron image in Fig. 2b) reveals a sharp concentration gradient of iron and oxygen, with a maximum concentration close to the outer surface of the host layer. The thickness of the porous Si layer containing iron is approx. 10 μm. This layer is observed as a bright region in the backscattered-electron image (Fig. 2b), due to the large difference in atomic number between iron and the other constituents of the film (silicon, oxygen, carbon, hydrogen, and the boron dopant for p-type silicon). Thus, the magnetite nanoparticles are solely infused into the large pores of the host layer. The backscattered-electron image of the encoding layer displays an alternating contrast pattern, arising from the density modulation produced by the periodic current waveform used in its preparation.

The magnetic properties of the porous Si microparticles were studied at room temperature by SQUID magnetometry (Fig. 3). The magnetization curve of magnetite-infused porous Si microparticles shows superparamagnetism similar to pure magnetite nanoparticles. The saturation magnetization of the magnetic porous Si microparticles is lower than that of the pure magnetite nanoparticles due to the lower concentration of magnetite nanoparticles in the diamagnetic porous Si matrix. To test this assertion, magnetite loading within the porous Si particles was determined by dissolving the porous Si host particles in ethanolic 5 M NaOH solution and weighing the residue. This gravimetric determination yields a weight percent of magnetite nanoparticles in the microparticles of ~32 %. This result is consistent with the SQUID data, which indicate magnetite content of ~29 wt % (calculated from the magnetization saturation values, Fig. 3).

Manipulation and Heating of Discrete Droplets

It was previously demonstrated that one-dimensional photonic crystals made from porous Si can be imparted with amphiphilic properties. These particles spontaneously assemble and orient at the interface between two immiscible fluids.[34] Adding magnetite to the particles endows them with the ability to be manipulated with magnetic fields, providing a means to direct the motion of liquid droplets in microfluidics applications.[25] In this study, the

superparamagnetic properties of the porous Si particles are utilized not only for manipulation but also for heat generation, by application of an alternating electromagnetic field. Thus, each layer of the amphiphilic magnetic particles has its specific function and the preferential location of these layers at the interface between the aqueous droplet and a surrounding organic liquid is of utmost importance. The particles are designed so that the magnetite host layer of the particles is hydrophilic and the encoding layer is hydrophobic. As a result, the particles align at the interface of an aqueous droplet immersed in oil with their magnetic layer facing the aqueous droplet and the encoding layer facing the organic phase. This self-assembly allows identification of the droplet using the spectrum of light reflected from the encoding layer and efficient heat transfer from the magnetic layer into the droplet.

In this study, different spectral codes are used to identify each of the two droplets containing a component of the FRET probe. Droplet 1 (D1) contains Cy3-conjugated oligonucleotides and the magnetic porous Si particles surrounding this droplet are characterized by a single spectral reflectance peak (Fig. 4a). Droplet 2 (D2) contains the Cy5-labeled oligonucleotides and is coated with particles characterized by a three-peak spectral code (Fig. 4a). The droplets were half-covered with magnetic porous Si particles in order to allow detection of the fluorescence from a FRET probe contained in the droplet using a cooled CCD detector, which will be discussed in the next section. The two droplets are merged by moving droplet 1 into a shallow well containing droplet 2 by means of a small rare-earth permanent magnet (Fig. 4a). After droplet fusion, the spectral code recorded from the particles covering the mixed droplet contains four peaks, resulting from a combination of the spectrum of the particles surrounding droplet 1 (one peak) and 2 (three peaks), Fig. 4b. The spectral ‘barcodes’ incorporated in the magnetic porous Si microparticles allow different droplets to be interrogated and identified in an ensemble of droplets. This approach is expected to be especially useful for performing complex bioassays containing multiple distinct liquid droplets and may be further developed with programmable control on a patterned magnetic surface.[38]

The magnetite nanoparticles infused within the porous Si microparticles can be heated by application of a radiofrequency electromagnetic field. A discrete aqueous droplet covered with magnetic porous Si microparticles and suspended in mineral oil was heated using a 338 kHz RF field of 3kW transmitted power. Fig. 5 depicts the temperature of the droplet vs. heating time. The temperature of the droplet increases from room temperature to 65 °C within 60 s, and a maximum temperature of more than 80 °C is reached after 300 s. At temperatures greater than 80 °C, gas bubbles are observed at the surface of the aqueous droplet, suggesting that the temperature in some regions of the droplet has exceeded the boiling point of water. A bare droplet (not covered with magnetic porous Si microparticles) suspended in mineral oil exhibits a temperature increase of only 5 °C after 300 s in the RF field. Similarly, a droplet surrounded by porous Si microparticles that contain little or no magnetite show ~5 °C temperature rise after 300 s in the RF field. These control experiments confirm that the temperature increase in the droplet is largely a result of heat generated in the magnetic porous Si microparticles covering the droplet. The small temperature increase observed in the control experiments can be attributed to resistive (Joule) heating of the coil surrounding the experimental dish and weak inductive heating of water subjected to the alternating electromagnetic field.

The heat generation mechanisms available to magnetic nanoparticles has been described in detail.[39–41] In the present case, the physical mechanism by which the magnetic porous Si particles are heated in the presence of the external alternating electromagnetic field is attributed to Néel relaxational losses that occur upon reorientation of the magnetic moments in the magnetite nanoparticles.[40] Inductive heating of the magnetic particles via eddy

currents may be neglected due to the low frequencies used.[42] The amount of heat generated in magnetic materials is strongly dependent on the particle size and microstructure as well as the applied field strength and frequency.[40,41,43,44] The amount of heating that can be obtained by hysteresis losses decreases dramatically as the particle radius decreases below 10 nm, whereas heating due to Néel relaxation becomes significant in this size regime.[41] The ability of the porous Si host to localize high concentrations of magnetite nanoparticles while maintaining their superparamagnetic properties allows heating at relatively low fields.

Fig. 6 depicts the effect of electromagnetic field strength on the droplet heating rate. At several values of coil current, power was applied for 30 s and the droplet temperature was measured immediately afterwards. As expected, the temperature of the droplet increases as the current in the RF coil (directly related to field strength) increases. This effect is more pronounced in the lower current range, where the temperature gradient between the droplet and the surroundings is small.

The time needed to reach the steady-state temperatures reported here is somewhat longer than desired for many microfluidic applications such as thermal cycling in PCR. The slow time to reach steady state is due to heat transfer to the oil (and room air) surrounding the droplet[45]—factors derived from the present experimental setup, which was not optimized for rapid cycling. In addition, the thermocouple used to measure temperature in Figs 5 and 6 has a significant thermal mass relative to the droplet being probed, and so the peak temperatures measured represent somewhat of an under-estimate. Additional factors, such as the amount of magnetic porous Si particles and the volume of oil, also affect the rate of temperature rise and thus can be used to tune the rate and the amount of droplet heating in a given experimental configuration.

FRET assay

Fluorescence resonance energy transfer (FRET) relies on the distance-dependent transfer of energy from a donor fluorophore to an acceptor fluorophore. Due to its sensitivity to distance, FRET has been used as a tool for measuring nanometer scale distances and changes in distances, both *in vitro* and *in vivo*.[46] The FRET technique is also used in biology as a nano-sized thermo-sensor to observe the heating of small areas by conjugating complementary oligonucleotides with FRET pair fluorophores.[42,47,48] This technique takes advantage of the temperature dependence of the reversible hybridization of oligonucleotides. In this study, complementary DNA strands were end-labeled with the donor-acceptor pair Cy3-Cy5. When allowed to hybridize, the close proximity of the dye molecules allows for FRET to occur, and upon excitation with blue (470 nm) light, red emission from Cy5 at 670 nm is observed. As the solution is heated and the duplex melts, the dyes separate. Emission from Cy3 is then observed at 570 nm, corresponding to a decrease in efficiency of the resonant energy transfer process. The relationship between the Cy5/Cy3 emission intensity ratio and temperature allows the fluorescence spectrum to be used to measure droplet temperature.

As described in the previous section, two droplets containing Cy3- and Cy5-conjugated complementary oligonucleotides were half-covered with magnetic porous Si microparticles. This half-coverage of the droplets by the particles allows better detection of fluorescence changes with the CCD detector. When the two droplets are merged at room temperature (Fig. 4b), hybridization of complementary oligonucleotides occurs. The merged droplet is then heated by application of an alternating electromagnetic field. The electromagnetic field is switched on for 25 s (5 s elapsed before maximum power was reached), and then off for 95 s. This cycle was repeated five times. The fluorescence spectra of the droplet during the heating process (Fig. 7a) display a change in the Cy5/Cy3 fluorescence intensity ratio with time. The temperature of the droplet was independently monitored by insertion of a

thermocouple probe before and after the heating intervals (Fig 7b). Since the calculated melting temperature of the FRET probe is 46.8 °C, the droplet temperature was cycled between 37 °C and 57 °C during the heating/cooling intervals. During heating, the Cy5/Cy3 intensity ratio decreases from a maximum value of ~1.5 (at ~37 °C) to a minimum value of ~0.5 (at ~57 °C). The reproducibility of the results during the five consecutive heating/cooling cycles demonstrates that the temperature of the droplet can be precisely controlled and the DNA duplex is durable enough to allow consistent hybridization and de-hybridization transitions in the presence of the magnetic porous Si microparticles. It is possible that some non-specific adsorption of the analytes to the microparticles occurs under the experimental conditions, although no evidence of this was found in the present study. The reproducibility of Cy5/Cy3 fluorescence intensity ratio over the five consecutive heating/cooling cycles indicates that non-specific adsorption of the DNA probes, if present, does not significantly impair the assay.

The temperature change measured by Cy5/Cy3 fluorescence intensity ratio correlates with the temperature measured with the external thermocouple probe (Fig. 8). Independent measurements on a particle/droplet assembly that was heated with a laboratory hotplate instead of with the RF coil produce the same correlation. With both heating methods, the Cy5/Cy3 fluorescence intensity ratio shows a similar decrease with increasing temperature.

Conclusions

This study demonstrates the feasibility of using encoded magnetic amphiphilic porous Si microparticles to locally heat, manipulate and identify discrete microliter-scale liquid droplets. The droplets in the present system can be heated and moved individually. As the level of heating is related to the amount of microparticles and their degree of magnetization, a group of discrete droplets can be simultaneously heated to different temperatures using a single coil. In addition, the one-dimensional photonic crystal etched into the porous Si particle provides a unique spectral code to identify a droplet. Thus the approach enables assays to be processed in any desired order in parallel fashion; for example in randomized or combinatorial arrays.

Furthermore, this droplet system overcomes a requirement of conventional conductive heating schemes – thermal contact between the heating element and reaction vessel. Thus, a chemical reaction requiring temperature control can be remotely actuated. The scheme potentially can be applied *in vivo*, using extracorporeal application of electromagnetic fields to activate and/or release therapeutic agents from inside a droplet.

Acknowledgments

This project has been funded in part with Federal funds from the National Cancer Institute of the National Institutes of Health (Contract No. N01-C0-37117) and the Air Force Office of Scientific Research (Grant# F49620-02-1-0288). M.J.S. and S.N.B. are members of the Moores UCSD Cancer Center and the UCSD NanoTUMOR Center under which this research was conducted and partially supported by NIH grant U54 CA 119335. J.P. thanks the Korea Science and Engineering Foundation (KOSEF) for a Graduate Study Abroad Scholarship. A.M.D. thanks the Graduate Research and Education in Adaptive Bio-Technology (GREAT) Training Program of the University of California Biotechnology Research and Education Program for a graduate fellowship. The authors thank Jason Dorvee, Sara Alvarez, and Dr. Greg Underhill for helpful discussions, and Evelyn York of the Scripps Institute of Oceanography, Analytical Instrument Facility, for assistance with the scanning electron microscopy measurements.

References

1. Delamarche E, Bernard A, Schmid H, Michel B, Biebuyck H. Science. 1997; 276:779–781. [PubMed: 9115199]

2. Kopp MU, de Mello AJ, Manz A. Science. 1998; 280:1046–1048. [PubMed: 9582111]
3. Schneegass I, Brautigam R, Kohler JM. Lab Chip. 2001; 1:42–49. [PubMed: 15100888]
4. Thorsen T, Maerkl SJ, Quake SR. Science. 2002; 298:580–584. [PubMed: 12351675]
5. DeMello AJ. Nature. 2003; 422:28–29. [PubMed: 12621418]
6. Hong JW, Quake SR. Nat Biotechnol. 2003; 21:1179–1183. [PubMed: 14520403]
7. Kotz KT, Noble KA, Faris GW. Appl Phys Lett. 2004; 85:2658–2660.
8. Pollack MG, Shenderov AD, Fair RB. Lab Chip. 2002; 2:96–101. [PubMed: 15100841]
9. Velev OD, Prevo BG, Bhatt KH. Nature. 2003; 426:515–516. [PubMed: 14654830]
10. Paik P, Pamula VK, Fair RB. Lab Chip. 2003; 3:253–259. [PubMed: 15007455]
11. Belder D. Angew Chem Int Ed. 2005; 44:3521–3522.
12. Chen DL, Gerdts CJ, Ismagilov RF. J Am Chem Soc. 2005; 127:9672–9673. [PubMed: 15998056]
13. Takeuchi S, Garstecki P, Weibel DB, Whitesides GM. Adv Mater. 2005; 17:1067–1072.
14. Burns MA, Mastrangelo CH, Sammarco TS, Man FP, Webster JR, Johnson BN, Foerster B, Jones D, Fields Y, Kaiser AR, Burke DT. Proc Natl Acad Sci U S A. 1996; 93:5556–5561. [PubMed: 8643614]
15. Ichimura K, Oh SK, Nakagawa M. Science. 2000; 288:1624–1626. [PubMed: 10834837]
16. Gallardo BS, Gupta VK, Eagerton FD, Jong LI, Craig VS, Shah RR, Abbott NL. Science. 1999; 283:57–60. [PubMed: 9872739]
17. Daniel S, Chaudhury MK, Chen JC. Science. 2001; 291:633–636. [PubMed: 11158672]
18. Kataoka DE, Troian SM. Nature. 1999; 402:794–797.
19. Hosokawa K, Fujii T, Endo I. Anal Chem. 1999; 71:4781–4785.
20. Choi SH, Newby BMZ. Langmuir. 2003; 19:7427–7435.
21. Jones TB, Gunji M, Washizu M, Feldman MJ. J Appl Phys. 2001; 89:1441–1448.
22. Atencia J, Beebe DJ. Nature. 2005; 437:648–655. [PubMed: 16193039]
23. Millman JR, Bhatt KH, Prevo BG, Velev OD. Nat Mater. 2005; 4:98–102. [PubMed: 15608646]
24. Kotz KT, Gu Y, Faris GW. J Am Chem Soc. 2005; 127:5736–5737. [PubMed: 15839641]
25. Dorvee JR, Derfus AM, Bhatia SN, Sailor MJ. Nature Mater. 2004; 3:896–899. [PubMed: 15531887]
26. Khandurina J, McKnight TE, Jacobson SC, Waters LC, Foote RS, Ramsey JM. Anal Chem. 2000; 72:2995–3000. [PubMed: 10905340]
27. Chan EM, Alivisatos AP, Mathies RA. J Am Chem Soc. 2005; 127:13854–13861. [PubMed: 16201806]
28. DeMello AJ, Habgood M, Lancaster NL, Welton T, Wootton RCR. Lab Chip. 2004; 4:417–419. [PubMed: 15472723]
29. Lagally ET, Simpson PC, Mathies RA. Sens Actuator B-Chem. 2000; 63:138–146.
30. Giordano BC, Ferrance J, Swedberg S, Huhmer AFR, Landers JP. Anal Biochem. 2001; 291:124–132. [PubMed: 11262165]
31. Kricka LJ, Wilding P. Anal Bioanal Chem. 2003; 377:820–825. [PubMed: 12925867]
32. Oda RP, Strausbauch MA, Huhmer AFR, Borson N, Jurrens SR, Craighead J, Wettstein PJ, Eckloff B, Kline B, Landers JP. Anal Chem. 1998; 70:4361–4368. [PubMed: 9796420]
33. Meade SO, Yoon MS, Ahn KH, Sailor MJ. Adv Mater. 2004; 16:1811–1814.
34. Link JR, Sailor MJ. Proc Nat Acad Sci. 2003; 100:10607–10610. [PubMed: 12947036]
35. Berger P, Adelman NB, Beckman KJ, Campbell DJ, Ellis AB, Lisensky GC. J Chem Educ. 1999; 76:943–948.
36. Cui Y, Bjork MT, Liddle JA, Sonnichsen C, Boussert B, Alivisatos AP. Nano Lett. 2004; 4:1093–1098.
37. Schnakenberg U, Benecke W, Lochel B, Ullerich S, Lange P. Sens Actuator A-Phys. 1991; 25:1–7.
38. Gunnarsson K, Roy PE, Felton S, Pihl J, Svedlindh P, Berner S, Lidbaum H, Oscarsson S. Adv Mater. 2005; 17:1730–1734.
39. Kalambur VS, Han B, Hammer BE, Shield TW, Bischof JC. Nanotechnology. 2005; 16:1221–1233.

40. Pankhurst QA, Connolly J, Jones SK, Dobson J. J Phys D-Appl Phys. 2003; 36:R167–R181.
41. Hergt R, Andra W, d'Ambly CG, Hilger I, Kaiser WA, Richter U, Schmidt HG. IEEE Trans Magn. 1998; 34:3745–3754.
42. Hamad-Schifferli K, Schwartz JJ, Santos AT, Zhang S, Jacobson JM. Nature. 2002; 415:152–155. [PubMed: 11805829]
43. Shinkai M. J Biosci Bioeng. 2002; 94:606–613. [PubMed: 16233357]
44. Berry CC, Curtis ASG. J Phys D-Appl Phys. 2003; 36:R198–R206.
45. Rabin Y. Int J Hyperthermia. 2002; 18:194–202. [PubMed: 12028637]
46. Selvin PR. Nat Struct Biol. 2000; 7:730–734. [PubMed: 10966639]
47. Jin RC, Wu GS, Li Z, Mirkin CA, Schatz GC. J Am Chem Soc. 2003; 125:1643–1654. [PubMed: 12568626]
48. Walker NJ. Science. 2002; 296:557–559. [PubMed: 11964485]

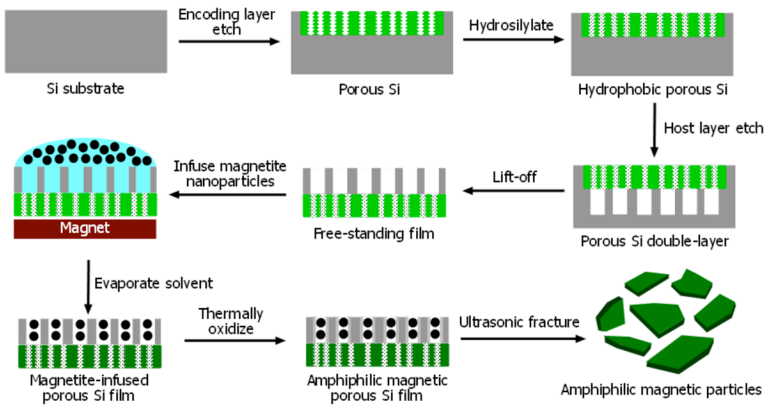

Figure 1.

Scheme showing the synthesis of magnetic amphiphilic porous Si microparticles. A spectral bar-code ("encoding layer") is first etched into the single-crystal Si substrate. The porous Si film is then hydrosilylated to generate a chemically stable hydrophobic layer. A porous host layer for magnetite loading is then etched into the substrate immediately beneath the encoding layer. The entire structure is then removed from the substrate by application of a current pulse. Magnetite nanoparticles are loaded into the porous host layer followed by thermal oxidation at low temperature to impart hydrophilic character to the magnetic layer. Finally, the magnetic film is placed in acetone and fractured into micrometer-sized particles by brief ultrasonication.

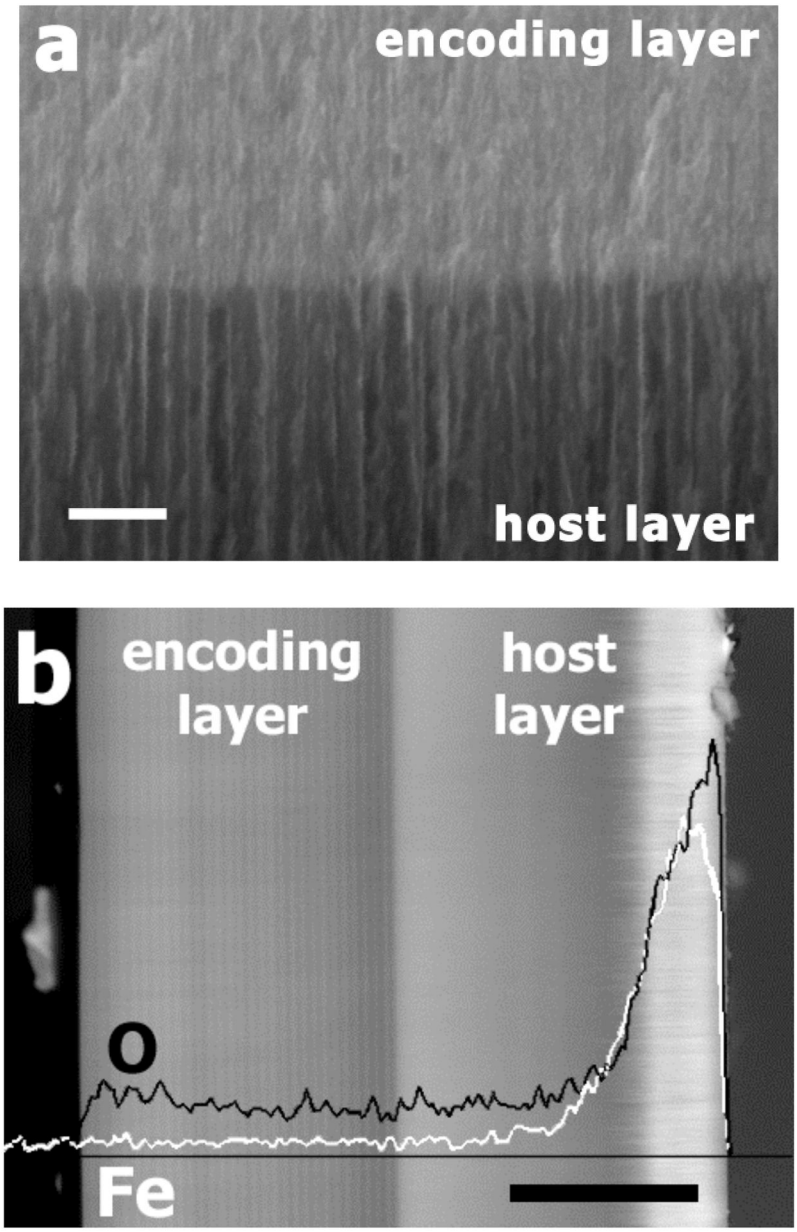

Figure 2.

Cross-sectional scanning electron micrographs of a magnetite-infused porous Si microparticle (“one-peak” preparation). **(a)** Secondary electron image of the interface between the encoding and the host layers. The encoding layer is prepared with a lower etching current (11.3–56.8 mA/cm^2), and possesses smaller pores than the host layer, prepared at a higher current density (303 mA/cm^2). Scale bar is 200 nm. **(b)** Back-scattered electron image with EDS line scan superimposed, showing the distribution of magnetite (iron oxide) in the particle. The black line in the image represents oxygen and the white line represents iron element maps. Scale bar is 20 μm.

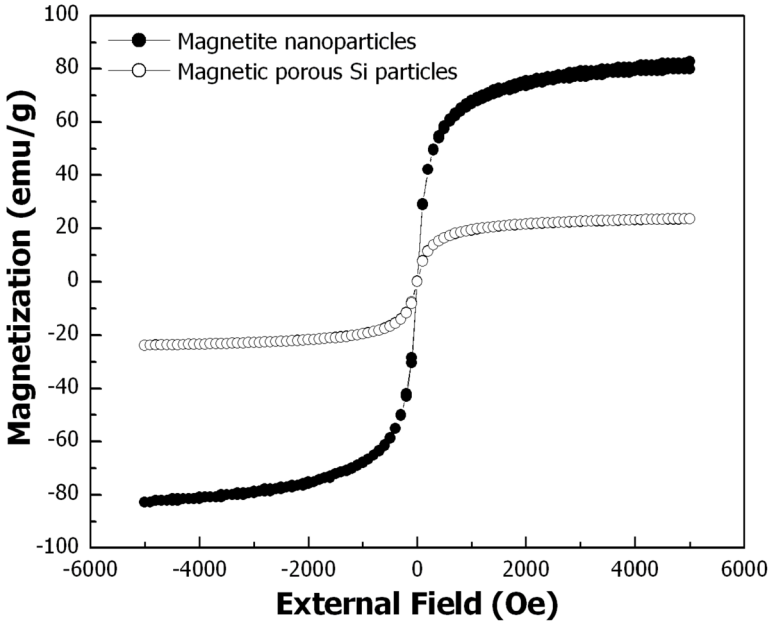

Figure 3.

Room-temperature magnetization curves of magnetite (Fe_3O_4) nanoparticles (●) and magnetite-infused porous Si microparticles (○). The magnetic porous Si microparticles display superparamagnetic behavior similar to magnetite nanoparticles, although the porous Si microparticles exhibit lower saturation magnetization on a per-gram basis due to the presence of diamagnetic porous Si.

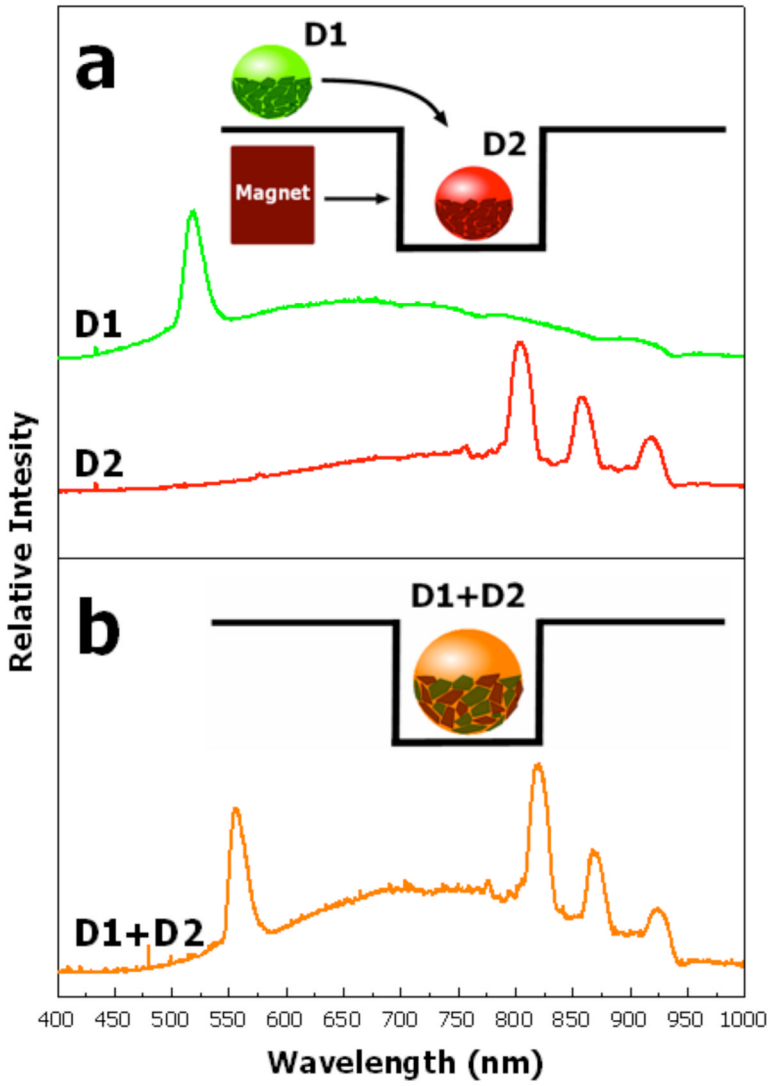

Figure 4.

Reflectivity spectra of magnetic porous Si microparticles surrounding aqueous droplets that contain fluorophore-conjugated oligonucleotides. **(a)** Reflectivity spectra obtained from the particles half-covering droplet 1 (D1), which contain Cy3-conjugated oligonucleotides, and the particles half-covering droplet 2 (D2), containing Cy5-conjugated oligonucleotides. The particles on D1 possess a spectral code consisting of one peak, while the particles on D2 carry a spectral code consisting of three peaks. The inset represents a schematic of the experimental setup used for manipulating the droplets. D1 is merged with D2, which is trapped a shallow well, using a magnet. **(b)** Reflectivity spectrum obtained after merging D1 and D2 shows the superposition of the two spectral codes from the two sets of particles. The inset represents a schematic of the experiment after merging D1 with D2.

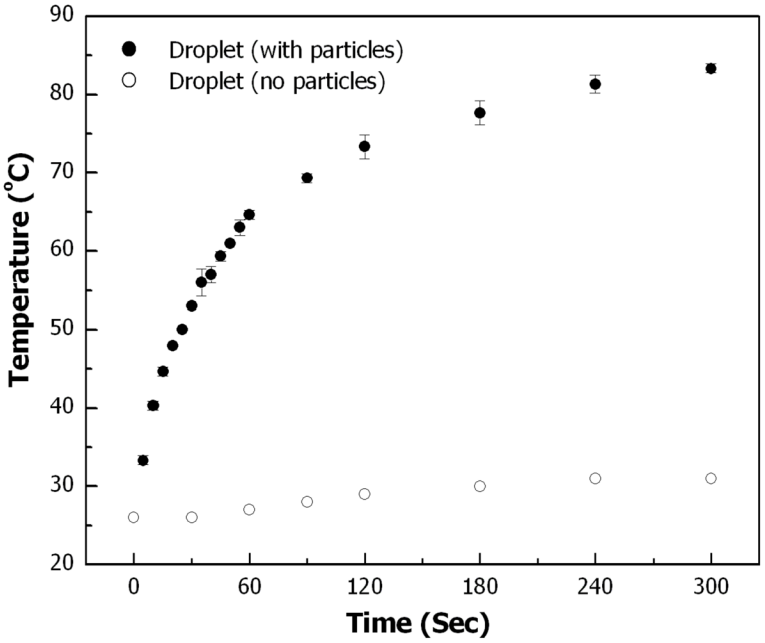

Figure 5.

Droplet temperature vs. heating time. A 50 μL droplet is placed in mineral oil and heated from 26 °C with an alternating electromagnetic field (3 kW). (●) A droplet covered with magnetic porous Si microparticles; (○) bare droplet (containing no particles). Droplet temperature is measured with a thermocouple probe immediately after the electromagnetic field is turned off. Each data point represents an average of three consecutive measurements.

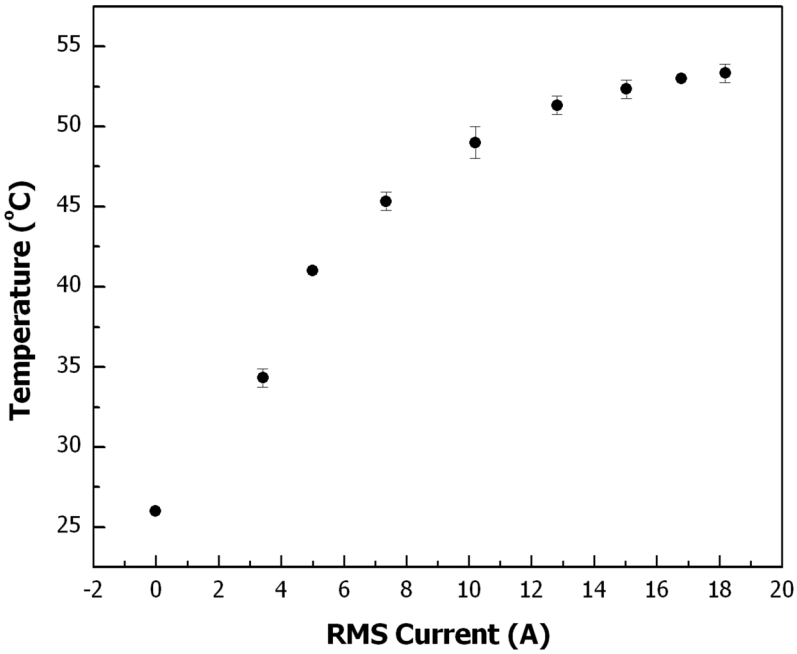

Figure 6.

Droplet temperature vs. RF coil current. A 50 μL aqueous droplet covered with magnetic porous Si microparticles is placed in mineral oil and heated from 26 °C with an alternating electromagnetic field for 30 s. Droplet temperature is measured immediately after the electromagnetic field is turned off. Each data point represents an average of three consecutive measurements. The coil current is expressed as the root-mean-square (or RMS) of the current sinusoid.

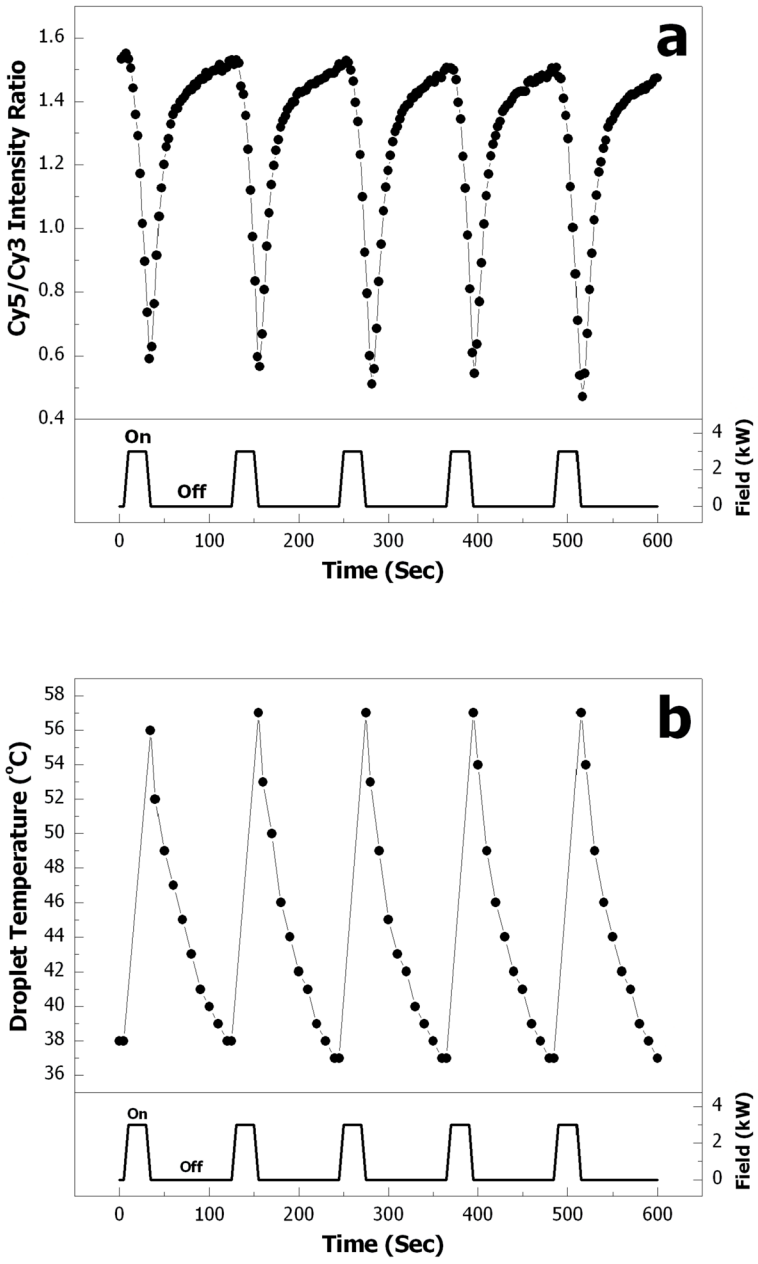

Figure 7.

Electromagnetic field-induced heating of a microparticle/droplet assembly leads to hybridization and de-hybridization of a FRET probe. **(a)** Change in Cy5/Cy3 fluorescence intensity ratio over five cycles of field application (on: 25 s and off: 95 s). Reproducibility of the curves indicates hybridization of the duplex is fully reversible. **(b)** Droplet temperature change over 5 cycles, measured with a thermocouple probe. For each data point, the temperature in the droplet is measured after the RF power is switched off.

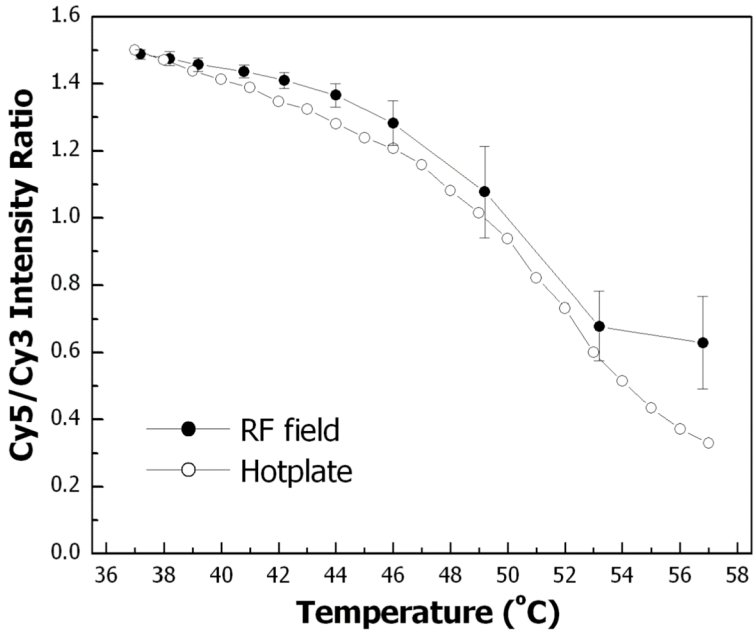

Figure 8.

Cy5/Cy3 fluorescence intensity ratio during droplet heating. (●) Heating achieved by application of RF electromagnetic field. (○) Heating achieved with a laboratory hotplate. A 50 μL droplet containing 0.6 nmol FRET probe is used in both experiments. RF field data is the average of the five heating/cooling cycles presented in Fig. 7.